POLYMER-PLASTICS TECHNOLOGY AND ENGINEERING
2017, VOL. 56, NO. 5, 543–555
http://dx.doi.org/10.1080/03602559.2016.1233260

Taylor & Francis
Taylor & Francis Group

Enhancement in Performance of Sulfonated PES Cation-Exchange Membrane by Introducing Pristine and Sulfonated Graphene Oxide Nanosheets Synthesized through Hummers and Staudenmaier Methods

Kobra Gerani, Hamid Reza Mortaheb, and Babak Mokhtarani

Petroleum Engineering Department, Chemistry and Chemical Engineering Research Center of Iran, Tehran, Iran

ABSTRACT

Sulfonated polyether sulfone-based cation-exchange membranes are prepared by incorporating different amounts of graphene oxide and sulfonated graphene oxide nanosheets. The graphene oxide nanosheets are synthesized according to Staudenmaier and Hummer methods and functionalized using 3-mercaptopropyl trimethoxysilane. Transport properties of nanocomposite membranes including ion-exchange capacity, transport number, and conductivity as well as their thermal stabilities are enhanced by incorporating sulfonated graphene oxide rather than graphene oxide. Also, the enhancement is more significant for the nanocomposites having functionalized graphene oxide synthesized by Staudenmaier method than those by Hummers method due to higher density of active sites in the Staudenmier graphene oxides for functionalization.

KEYWORDS

Cation-exchange membrane; Hummers method; Staudenmaier method; sulfonated graphene oxide; sulfonated polyether sulfone; transport properties

GRAPHICAL ABSTRACT

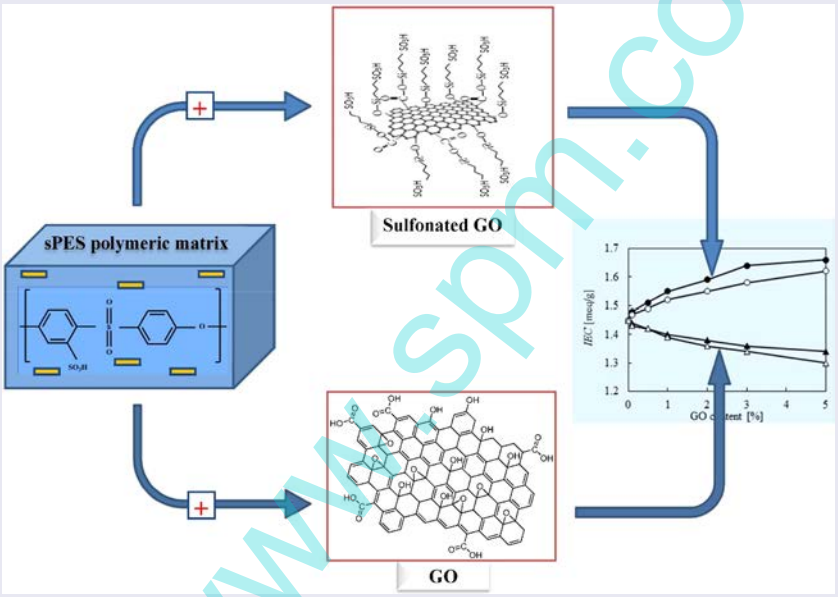

Introduction

Ion-exchange membranes (IEMs) are widely investigated and used in various separation applications such as desalination of seawater and treatment of industrial wastewaters. An IEM allows some specific ions, i.e., "counterions" to permeate through the membrane and prevents some other "co-ions", which has the same charge as the fixed ions in the membrane matrix[1–3]. The most expected property of an ion-exchange membrane is its high permselectivity, i.e., high permeability to counterions while being impermeable to co-ions, and having low electrical resistance and good mechanical/chemical stabilities[4,5]. On the other hand, fossil fuel restrictions[6] have created large interests for investigations of alternative energy resources such as fuel cell technology, in which chemical energy stored in the

CONTACT Hamid Reza Mortaheb mortaheb@ccerci.ac.ir Petroleum Engineering Department, Chemistry and Chemical Engineering Research Center of Iran, P.O. Box 14335-186, Tehran, Iran.
Color versions of one or more of the figures in this article can be found online at www.tandfonline.com/lpte.

chemical bonds of H_2 and O_2 are converted into electricity[7–10]. Since proton-exchange membranes (PEMs) are the major components in the fuel cells, researches are concentrated to find membranes with excellent properties[11–15]. A commercial membrane which is available for use in this process is Nafion due to its chemical stability and high conductivity. However, the high cost of the membrane and methanol crossover restrict its usage. The researches are then focused on the development of inexpensive and high-performing membrane materials such as polyether sulfone)PES for PEM fuel cells[16].

Ion-exchange membranes are also used in electrodialysis, in which ion-exchange membranes separate ionic species from an aqueous solution and other uncharged components by inducing an electrical potential[17–20]. As a suitable approach for overcoming the problems of proton conductivity at high temperatures, incorporating inorganic particles into the membranes to increase their water retention and proton conduction is interested in many researches[11,21]. The properties depend on particle type, size, shape, concentration, and also interactions between the matrix and nanoparticles[5,22–25]. Functionalization of particles can enhance their interaction with the polymeric matrix and uniform distribution[26–28]. Graphene-based materials have exhibited great potentials in various fields such as physics, chemistry, biology, and electronics due to their unique electronic properties, the facile synthesis, and the ease of functionalization[29]. Graphene oxide (GO) is derived from graphene by various chemical oxidation methods. It is characterized by its large specific surface area and layered structure having significant amounts of oxygen containing groups such as hydroxyl, carboxyl, and epoxide on its basal plane and edges that can be functionalized thorugh covalent or noncovalent bonding[30]. The high surface area and good thermal properties of GO makes it appropriate for many applications. Surface modifications of GO by introducing functional groups improve its surface interaction and make it appropriate for special tasks such as introducing in the IEMs[31–37]. In this study, graphene oxide is prepared by two different methods and is functionalized by a sulfonating agent. The produced graphene oxide derivatives are introduced into PES to make nanocomposite membranes with different filler contents. The surface morphology, thermal stability, water uptake, transport properties, and ionic conductivity of the synthesized membranes are then investigated.

Experimental

Material

Polyether sulfone (Ultrason E6020P, $M_w = 51{,}000$) was purchased from BASF Chemical Co. (Germany) and used after drying under vacuum. 3-mercaptopropyl trimethoxysilane (MPTMS) was purchased from Merck (Germany). Concentrated sulfuric acid (95–98%), hydrogen peroxide (30%), hydrochloric acid (36%), and potassium permanganate were purchased from Merck (Germany) and used as they received. Natural graphite powder and other chemicals were obtained commercially and used without further purifications.

Sulfonation reaction of polyether sulfone

Polyether sulfone was sulfonated by chlorosulfonic acid according to the procedure in the literature[38]. In the first step, PES was dissolved in sulfuric acid to obtain a homogeneous mixture. Chlorosulfonic acid as the sulfonating agent was then added dropwise to the solution under continuous mechanical agitation at room temperature. The reaction was performed for 5 h at room temperature. The weight ratio of PES, sulfuric acid, and chlorosulfonic acid was 3:30:17, respectively. The precipitates were filtered and washed several times with deionized water and finally were dried in a vacuum oven at 70°C.

Synthesis of graphene oxide

Figure 1 shows the structure of graphene oxide[39]. Synthesis of graphene oxide is mainly performed by oxidation of graphite through two methods of Hummers and Staudenmaier as described below.

Synthesis of graphene oxide by Hummers method

The graphene oxide was prepared from natural graphite flakes by Hummers method as reported in the literature[40]. Graphite powder (2 g) and sodium nitrate (1 g) were mixed with 46 ml of concentrated sulfuric acid (98%) in a round-bottom flask. The entire process was performed in an ice bath under constant stirring. Potassium permanganate (6 g) was then added slowly

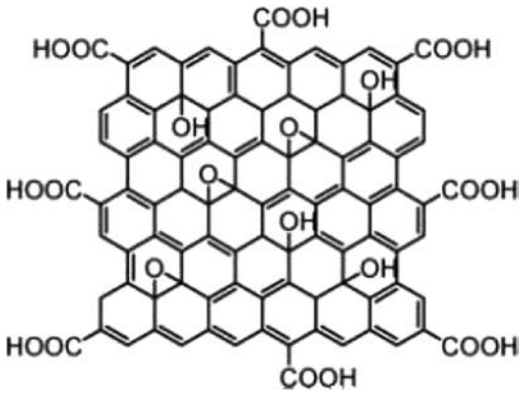

Figure 1. Structure of graphene oxide.

to the slurry as the oxidizing agent at a temperature lower than 20°C and was thoroughly mixed. The mixture was then stirred for 1 h at room temperature. A total of 92 ml of distilled water was added drop by drop to the mixture and was kept for 60 min under ultrasonic waves. The reaction mixture was then diluted with 280 ml of distillated water. H_2O_2 (30%) was then added to neutralize the remaining potassium permanganate[36].

The deposit was washed with large amounts of water and HCl (10%). Excess HCl was removed by centrifuging for several times. The product was then collected and dried in an oven at 70°C overnight.

Synthesis of graphene oxide by Staudenmaier method

Two grams of graphite powder was mixed with 36 ml of concentrated sulfuric acid (98%) and 18 ml of nitric acid (68%) in a round-bottom flask. The entire process was performed in an ice bath under constant stirring. A total of 22 g of potassium chlorate, $KClO_3$, was then added slowly to the slurry for 2 h. After thorough mixing, the mixture was removed from the ice bath and stirred for 1 week at room temperature. A total of 300 ml of distilled water was added drop by drop and the mixture that was kept for 2 h under ultrasonic agitation. The deposit was then washed with a large amount of water and was centrifuged several times to remove excess acids. The collected deposit was then dried in the oven at 70°C[41].

Functionalization of graphene oxide

The synthesized graphene oxides were functionalized using MPTMS as the sulfonic acid group precursor. The synthesized GO in either of the previous steps was dispersed in dried toluene and sonicated for about 20 min. MPTMS was added into the mixture and the reaction was performed under total reflux at 110°C for 24 h. Hydrogen peroxide (30%) was added after reducing temperature to room conditions and the mixture was stirred for 24 h. The precipitate was washed several times with ethanol and water. It was centrifuged and dried overnight in the oven at 70°C[36].

The procedures for GO synthesis and functionalization are demonstrated in Figure 2.

Preparation of composite membranes

The composite membranes were prepared using solvent evaporation technique. The nanosheets were dispersed in dimethylacetamide by sonication while the polymeric matrix was separately dissolved in the solvent. The uniform solutions were then mixed together and stirred at 50°C. The mixture was then sonicated for 2 h and the bubbles were removed. The obtained viscous solution was cast by a doctor blade on a flat surface glass and dried in the vacuum oven (12 h at 70°C and 8 h at 90°C). The composite membrane was then protonated by immersing in a 1 M HCl solution for 24 h and

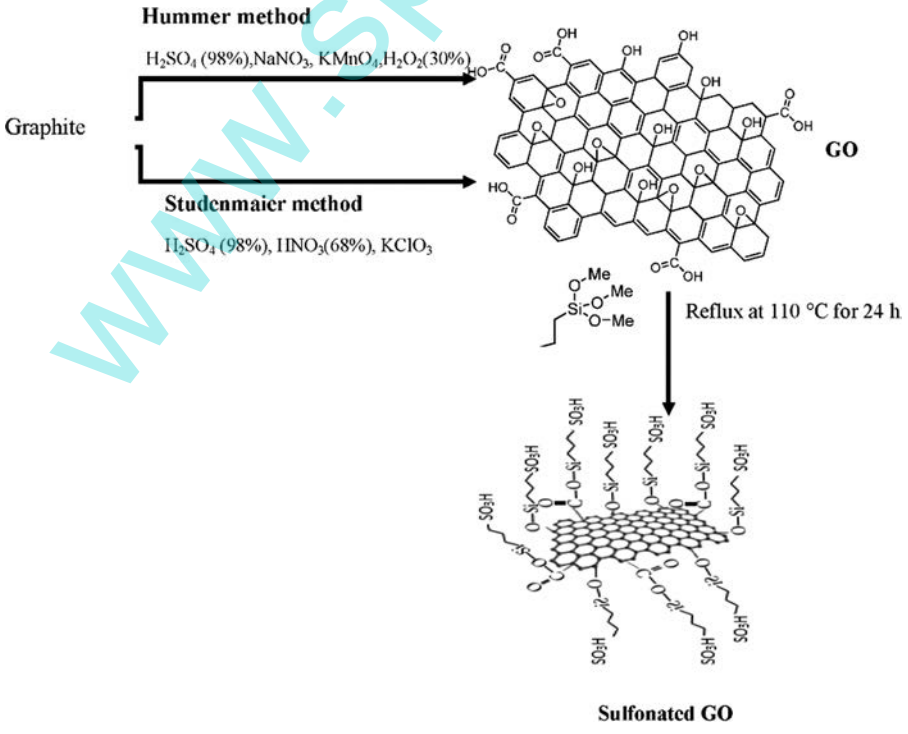

Figure 2. GO synthesis and sulfonation reaction.

Table 1. Labeling of membranes in present research.

		Synthesis method*	
		Staudenmaier	Hummers
Filler type	GO	mGOS-*x*	mGOH-*x*
	Functionalized GO	mfGOS-*x*	mfGOH-*x*
Without filler		sPES	

sPES, sulfonated polyether sulfone.
*x is the weight percent of filler in the composite membrane.

washing several times with deionized water. The membranes with different contents of synthesized GO or sulfonated GO (fGO) (0, 0.1, 0.5, 1, 2, 3, and 5 wt%) were prepared and labeled as indicated in Table 1 where x is filler content (wt%) in the composite membrane.

Characterization of the membranes

Fourier transform infrared spectrophotometry

The structures of synthesized graphene oxides and composite membranes were investigated by a Perkin Elmer 883 FTIR spectrophotometer in the wave number range of 4,000–400 cm^{-1} at 25°C. The membrane samples were dissolved in dichloromethane for placement on KBr pellets.

Membrane morphology

The structural characteristics of the fillers and the synthesized membranes were determined by using X-ray diffraction (XRD, Bruker AXS, D8-advance, $2\theta = 4$–70, $k = 0.71$ Å) where the morphologies of the membranes were studied by scanning electron microscopy (SEM, JSM-840A) and atomic force microscopy (AFM, CSPM 75 5000). The membrane samples were snapped in liquid nitrogen to get a sharp cross-sectional surface image. AFM was used also to determine the number of graphene oxide layers. The sample was prepared by sonication of graphene oxide in water and then adding one drop of sample on a surface of mica, which was washed with distilled water and dried for 24 h in ambient conditions before hand.

Thermal stability

The degradation process and thermal stability of graphene oxides and the synthesized membranes were investigated using thermogravimetric analysis (TGA, NETZSCH, Germany) under a nitrogen atmosphere using a heating rate of 10°C min^{-1} in the range of 25–800°C.

Ion-exchange capacity and water uptake

Ion-exchange capacity (IEC) of the membrane was determined using titration method by standard solutions of HCl, NaCl, and NaOH. Phenolphthalein was used as the indicator. The membrane sample was immersed in 1 M HCL and washed with distilled water until excess acid was removed. The sample was equilibrated in 1 M NaCl solution for 24 h under stirring at ambient temperature and then titrated by a 0.01 M solution of NaOH. The ion-exchange capacity was calculated as follows:

$$\mathrm{IEC} = \frac{\text{consumed volume of solution (ml)} \times 0.01\ \text{(eq/1)}}{\text{weight of dried membrane (g)}}\ [\text{meq/g}] \tag{1}$$

The water uptake (φ_w) was calculated to characterize the capability of water retention in the ion-exchange membrane. The membrane was first dried at 80°C for 24 h and weighed (W_{dry}). It was then soaked in de-ionized water at room temperature for 24 h. The excess water on the surface of the membrane was removed before determining the wet weight of the membrane (W_{wet}). The water uptake was calculated as follows:

$$\varphi_w = \frac{W_{wet} - W_{dry}}{W_{dry}}[-] \tag{2}$$

Membrane potential, transport number, and permselectivity

The membrane potential (E_m) was evaluated by using two horizontal chambers filled with NaCl solutions with different concentrations (0.01 and 0.1 M) and separated by the membrane. The setup was placed on a stirrer and the solutions were mixed by magnets in the chambers. The potential difference across the membrane was determined using a digital multimeter connected to two Ag/AgCl electrodes in the chambers. The membrane was equilibrated with deionized water before measurement. The membrane transport number (t_c^m), as a characteristic index of membrane selectivity, depends on the concentrations of external solutions and the ion-exchange groups in the membrane. It was estimated from the membrane potential using Teorell, Meyer, and Sievers approach as follows[42]:

$$E_m = \frac{RT}{F}(2\,t_c^m - 1)\ln\left(\frac{c1}{c2}\right) \quad [v] \tag{3}$$

where c_1 and c_2 are the mean concentrations of electrolytic solutions, R is the universal gas constant

(8.314 J K^{-1} mol^{-1}), F is the Faraday constant (96,485.3 C mol^{-1}), and T is the absolute temperature (K).

The ion selectivity of the membrane is expressed in terms of membrane permselectivity, P_s, and the concentration of fixed charges on the membrane surface, X_m, as follows:

$$P_s = \frac{t_c^m - t_c}{1 - t_c} \quad [-] \tag{4}$$

$$X_m = \frac{2\,C_s\,P_s}{\sqrt{1 - P_s^2}} \quad [\text{mol dm}^{-3}] \tag{5}$$

where t_c is the counterion transport number in the solution phase (approximately 0.39 for sodium ion in a sodium chloride solution at 25°C) and C_s is the mean electrolyte concentration (mol dm^{-3}).

Membrane ionic conductivity

Measurements of membrane conductance were accomplished using a clip cell. Before the experiments, the membrane was soaked in a 0.5 M NaCl solution. The resistance of membrane was measured at room temperature by the potentiostat/galvanostat frequency response analyzer (Auto Lab, Model PGSTAT 30) in a frequency range of 0.1–100 kHz with an oscillating voltage of 10 mV amplitude. The membrane resistance (R_m), equilibrated in the electrolyte solutions, was calculated by subtracting electrolyte resistance (R_{sol}) in the clip cell (without an inserted membrane) from the total cell resistance (R_{cell}), $R_m = R_{cell} - R_{sol}$. The conductivity of membrane was determined from the following equation:

$$\sigma = \frac{L}{A \cdot R_m} \quad [\text{S cm}^{-1}] \tag{6}$$

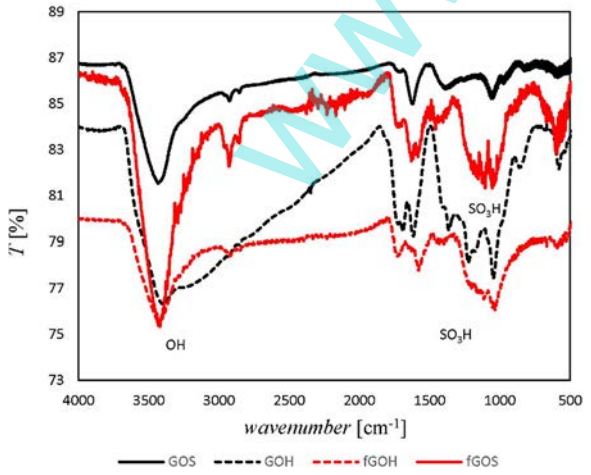

Figure 3. FTIR spectra of GO synthesized by Hummers and Staudenmaier methods and their corresponded functionalized GOs. *Note:* FTIR, Fourier transform infrared.

where A is the membrane cross-sectional area and L is the distance between the electrodes.

Results and discussion

Structural characterization of GO nanosheets

Fourier transform infrared spectroscopy characterization

Fourier transform infrared (FTIR) spectra of GO and functionalized GO by Hummers (Staudenmaier) method are represented in Figure 3. The FTIR spectra of GO represent peaks at 3,394 (3,435) cm^{-1} (O–H stretching vibrations), at 1,700 (1,732) cm^{-1} (stretching vibrations from C = O), at 1,615 (1,623) cm^{-1} (skeletal vibrations from unoxidized graphitic domains), at 1,360 (1,391) cm^{-1} (C–OH stretching vibrations), at 1,225 (1,263) cm^{-1} (C–O–C), and at 1,048 (1,036) cm^{-1} (C–O stretching vibrations). The presence of all these characteristic absorption peaks in FTIR results confirms that functional groups were introduced onto the surface of graphite by both Hummers and Staudenmaier methods.

Fourier transform infrared spectra of GO after sulfonation have been also shown in Figure 3. Their difference with the aforementioned spectra for GO is the addition of a new peak at 1,212, 1,149 (1,130) cm^{-1} that is attributed to the absorption of sulfonic acid group ($-SO_3H$)[43,44].

Thermal properties of GO nanosheets

The results of TGA for the synthesized fillers and the differential thermogravimetric curves of these samples are shown in Figure 4a and b, respectively. It can be seen that the weight losses of the GO synthesized by Hummers method in heating up to 600°C is 41% while that of GO synthesized by Staudenmaier method is 39%. The weight losses of their corresponded functionalized graphene oxides are 29 and 26%, respectively.

As expected, the weight losses from room temperature to 150°C is attributed to the absorbed and bounded water, while significant decrease from 50 to 250°C is caused by pyrolysis of the oxygen-containing functional groups such as carboxylic acid and alcohol on GO because of their easy decomposition[44]. The functionalized graphene oxides show enhanced thermal stabilities, i.e., a shifted degradation to higher temperatures due to existence of more functional groups in their structures. The weight losses of functionalized GOs at 380°C are due to the decomposition of sulfonic acid groups. The percentages of weight loss for the functional groups on GO are lower than those of functionalized GO. This can be attributed to the reduction of

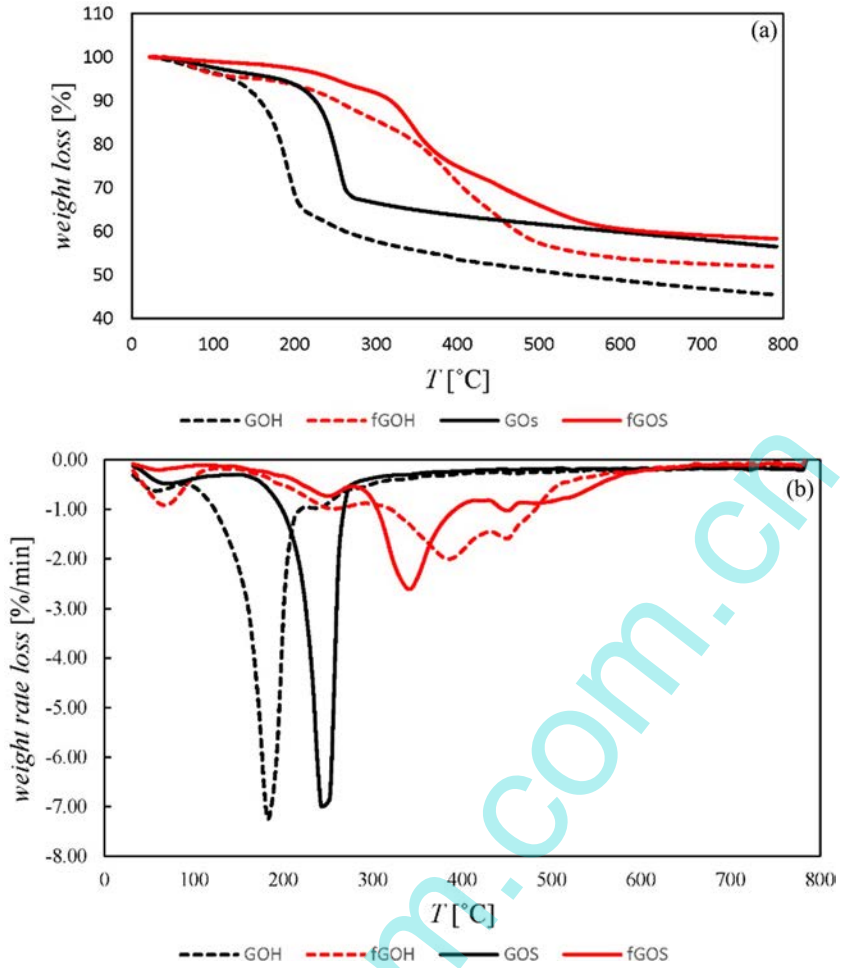

Figure 4. (a) TGA and (b) DTG spectra of GOs synthesized by Hummers and Staudenmaier methods and their corresponded functionalized GOs. *Note:* TGA, thermogravimetric analysis; DTG, differential thermogravimetric.

thermally unstable oxygenated functional groups on the functionalized GO samples[45].

X-ray diffraction analysis of GO nanosheets

The XRD patterns obtained for as-synthesized GOs by Hummers and Staudenmaier methods are shown in Figure 5. They represent diffraction peaks at $2\theta = 12.93°$ and 12.54°, respectively. The diffraction peak of pure graphite based on literature is around 26°[46]. The disappearance of the peak at 12° confirms that the GOs are completely oxidized after the chemicaloxidation and exfoliation[47].

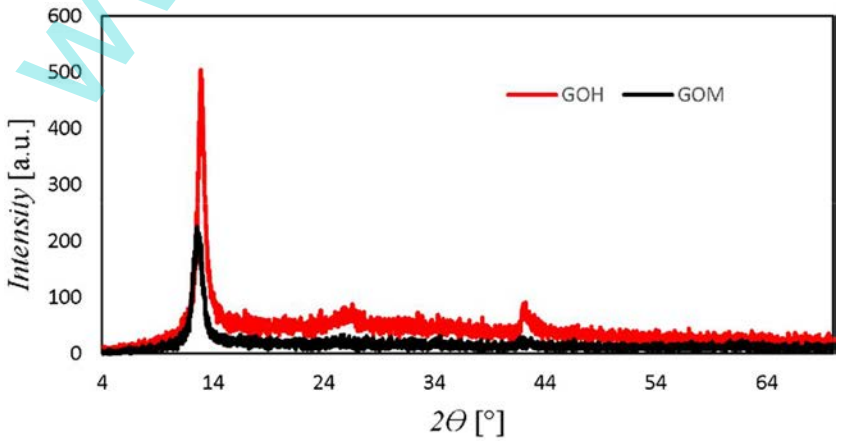

Figure 5. X-ray diffraction patterns of GOs synthesized by Hummers and Staudenmaier methods.

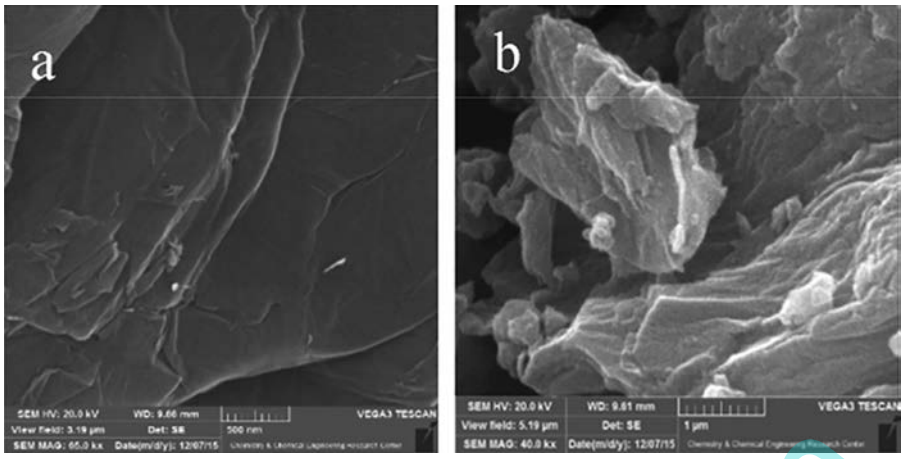

Figure 6. SEM images of (a) GO (65,000×) and (b) functionalized GO (40,000×) nanosheets synthesized by Hummers method.

Morphology of synthesized GO nanosheets

The SEM images of the synthesized GO and functionalized GO nanosheets by the Hummers method are shown in Figure 6. The images represent a layered and wrinkled sheet-like two-dimensional structure of graphene oxide. The distance between the layers and thin edges can be seen in the images. Oxidized graphene sheets are relatively large and the structure is like a thin screen. The surface of functionalized GO shows a relatively higher roughness compared to that of the GO.

The degree of exfoliation and thickness distribution of GO nanosheets can be investigated by AFM. The three-dimensional AFM image of an individual GO nanosheet synthesized by Staudenmaier method is shown in Figure 7. As seen in the figure, the thickness of synthesized nanosheet is about 1–2 nm, which is in the range of thickness for one layer of GO and confirms

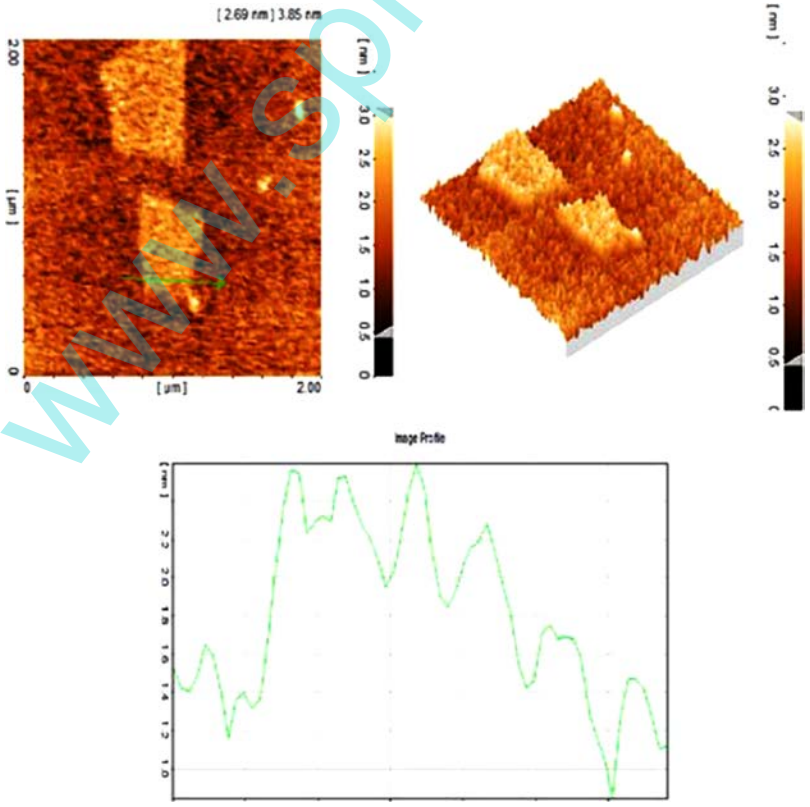

Figure 7. AFM pattern of GO synthesized by Staudenmaier method. *Note:* AFM, atomic force microscopy.

that GO has been successfully exfoliated. The thickness of GO nanosheets is higher than that of graphene due to the presence of oxygen-containing functional groups on their both sides. The lateral dimensions vary between 0.4 and 1 μm. The observed atomic scale roughness is due to structural defects caused by oxidation on graphene. The GO sheets are expected to be thicker due to the presence of covalently bonded oxygen and slight displacement of sp^3-hybridized carbon atoms above and below the original graphene plane[48]. The carbon–oxygen bonds partially change the carbon atoms' hybridization from sp^2 to sp^3 and arrangement of graphene layers into turbostratic (locally parallel) structure[49].

Characterization of polymer composite membranes

Fourier-transformed infrared spectrum of membranes

Figure 8 shows the FTIR spectra of sulfonated PES (sPES) and composite membranes. The introduction of sulfonic acid groups was confirmed by the FTIR spectra. The peaks at 1,735 and 1,629 cm^{-1} in absorption bands of sPES polymer are attributed to vibration of aromatic-cring skeleton. The two absorption peaks at 1,153 and 1,108 cm^{-1} are characteristics of aromatic SO_3^- stretching vibrations. The peak for aryl oxide appears at 1,239 cm^{-1}. The O–H stretching absorption peak between 3,000 and 3,500 cm^{-1} in the FTIR spectra of the membrane indicates the existence of hydrogen bonding. The presence of aliphatic CH is indicated by the band stretching from 2,900 to 3,000 cm^{-1}.

All of the expected functional groups of the sPES backbone structure are observed in the spectra of composite membranes. However, the typical peaks of GO and functionalized GO cannot be observed because these peaks overlap with the characteristic peaks of sPES due to the their low doping amounts (2 wt%)[31,50].

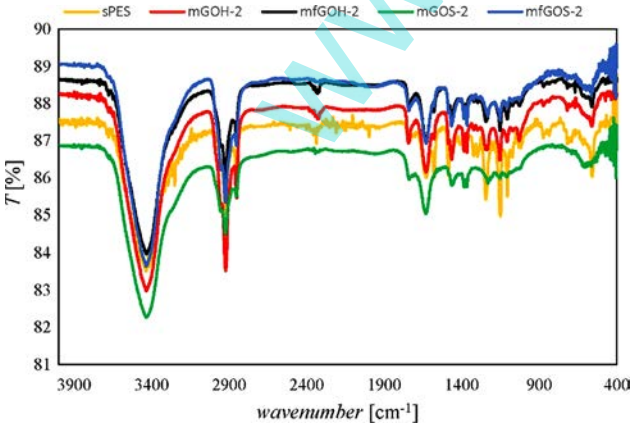

Figure 8. FTIR spectra of sPES and composite membranes having GO synthesized by Staudenmaier and Hummers methods. *Note:* FTIR, Fourier transform infrared.

Morphology of membranes

Scanning electron microscopy images from surfaces and cross sections of membranes are shown in Figure 9. Although in comparison to the sPES membrane, the surfaces of nanocomposite membranes have higher roughnesses, they represent relatively smooth surface where no accumulation of graphene oxide nanosheets are observed. The graphene oxide nanosheets are well dispersed in the sPES polymeric matrix because of their carbonaceous structure.

The cross-sectional SEM images also represent a homogeneous and layered structure of the nanocomposite membranes due to strong interfacial adhesion and good compatibility of GO nanosheets and the sPES matrix. This result is reasonably attributed to the fact that the oxygen-containing groups on the GO surface result in a strong electrostatic attraction (such as hydrogen bonds) between GO and sPES. The layered structure of nanocomposite membranes can facilitate proton conductivity in parallel paths and channels to create more proton transfer and adsorb more water to improve the performance of composite membranes.

The homogeneous dark color appearance of the composite membranes having fGO in their matrices indicates the successfulness of GO sulfonation. The cross-sectional SEM images of fGO nanocomposite membranes are also shown in Figure 9. The fillers are homogeneously distributed in the sPES matrix without causing any structural defect.

The SEM images confirm that the nanocomposites prepared using GO and functionalized GO synthesized by Staudenmaier method have a more dense and uniform structure than those prepared using GO and functionalized GO synthesized by Hummers method.

Thermal stability of composite membrane

The thermogravimetric analyses of nanocomposite membranes are shown in Figure 10. The figure shows that sPES membrane has three distinct degradation steps; the first weight loss (about 5%) is seen from room temperature to about 100°C due to evaporation of adsorbed water, the second one from 250 to 400°C is attributed to thermal degradation of sulfonic acid groups, and the third one above 450°C is due to the thermal decomposition of the main sPES chains. Similar steps are seen in the TGA curves of composite membranes with a shift in temperature range. The composite membranes' second weight loss in the range of 300–400°C is due to degradation of sulfonic acid groups of the polymeric matrix and oxygen-containing

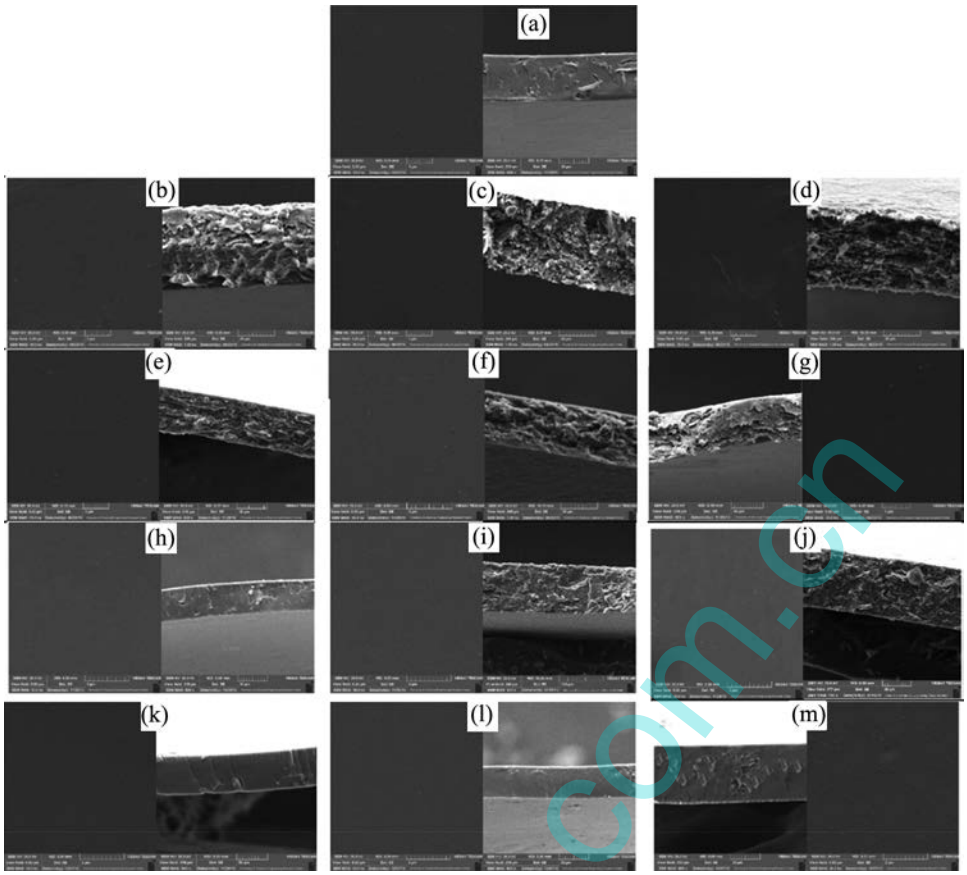

Figure 9. Surface and cross-sectional images of (a) sPES, (b) mGOH-0.5, (c) mGOH-1, (d) mGOH-2, (e) mfGOH-0.5, (f) mfGOH-1, (g) mfGOH-2, (h) mGOS-1, (i) mGOS-2, (j) mGOS-3, (k) mfGOS-1, (l) mfGOS-2, and (m) mfGOS-3.

functional groups on the nanosheets. A more thermal stability is afforded for the nanocomposite membrane having functionalized GO due to interaction between sulfonic groups of the functionalized GO nanosheets and the sulfonic groups of the polymeric matrix.

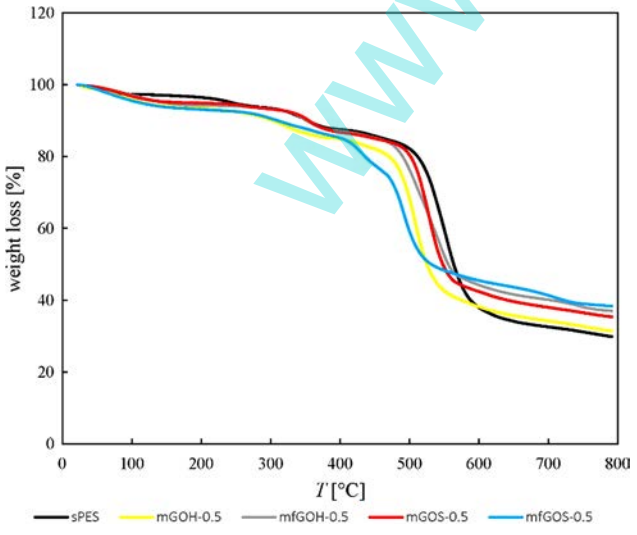

Figure 10. TGA thermographs for sPES and composite membranes. *Note:* TGA, thermogravimetric analysis.

Ion-exchange capacity of composite membranes

The ion-exchange capacities of composite membranes having GO and functionalized GO synthesized by both Staudenmaier and Hummers methods are shown in Figure 11. IEC represents the concentration of sulfonic

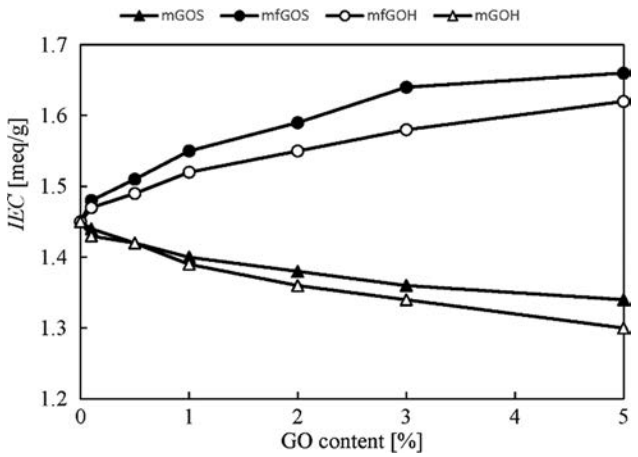

Figure 11. IEC of composite membranes having GO synthesized by Staudenmaier and Hummers methods. IEC, ion-exchange capacity.

acid groups and thus the charged nature of the ion-exchange membranes, which play an important role in proton conductivity. IEC values of nanocomposite membranes are reduced compared to sPES membrane because incorporating neutral GO decreases the density of sulfonic acid groups in the polymer. However, as shown in Figure 11, IEC of functionalized GO composite membranes, which have negative charges due to the presence of sulfonic acid groups in their structure, increases by increasing the filler content. Meanwhile, the figure reveals that the IEC of membrane having Staudenmaier GO is higher than that of membrane having Hummers GO at the same content (max. 3% at 5 wt%). The figure also reveals that the increment in IEC is more significant (in the range of 0.7–3.8%) for the composite membranes having Staudenmaier functionalized GO than those having Hummers functionalized GO. This is because of positioning more active sites in the structure of GO synthesized by Staudenmaier method, which are replaced by sulfonic acid groups in the functionalization step.

Water uptake of composite membranes

The water uptake (φ_w) of the composite membranes having GO and functionalized GO synthesized by both Staudenmaier and Hummers methods are shown in Figure 12. As can be seen in the figure, φ_w increases by increasing GO content due to hydrophilic characteristic of GO nanosheets. The higher hydrophilicity of sulfonic acid groups makes the composite membranes having functionalized GO more hydrophile and resulting in enhance in their water uptakes.

Similar to the trend observed in IEC, the water uptakes of the composite membranes having Staudenmaier GO and correspondingly functionalized Staudenmaier GO are higher (up to 15%) than those of the membranes having Hummers GO.

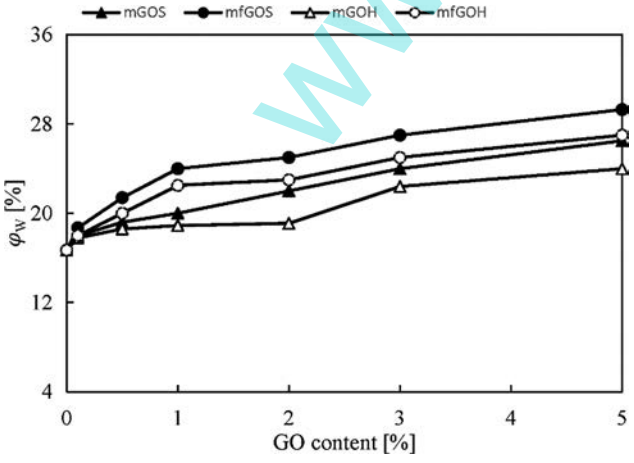

Figure 12. Water uptakes of composite membranes having GO synthesized by Staudenmaier and Hummers methods.

Transport number and permselectivity

The permselectivity of membrane for transporting counterions with different mobilities induces an electrical potential difference when two electrolyte solutions with different concentrations are separated by the membrane. The membrane potential data in NaCl solutions were obtained for all the membranes as presented in Table 2 in terms of transport number and permselectivity. It can be seen that the membrane potential, transport number, and permselectivity are improved using GO nanosheets (up to 5 wt%) and the enhancement order is as follows: mfGOS > mfGOH > mGOS > mGOH > sPES, i.e., the nanocomposite membranes having functionalized GO have better results that those having GO, and that the nanocomposite membranes having synthesized GO by Staudenmaier method have better transport properties than those having synthesized GO by Hummers method. Basically, the adsorptive characteristic and ionic transport properties of applied GO nanosheets, which provide more conducting regions for the GO nanocomposite membranes, result in their enhanced transport properties. The high specific surface area of nanosheets is also beneficial for diffusion of ions from the solution onto the active sites of nanosheet surface in the membrane matrix that improves the accessibility of ion-exchange functional groups in the membrane matrix. This makes better Donnan exclusion that is responsible for increasing membrane potential, transport number, and selectivity[51]. GO and functionalized GO control the pathways of ions because the flow

Table 2. Transport number, permselectivity, and concentration of fixed charges on membrane surface having (a) GO and (b) functionalized GO nanosheets.

GO synthesis method							
Hummers				Staudenmaier			
Filler content	t_c^m (–)	P_s (–)	X_m (mol dm^{-3})	Filler content	t_c^m (–)	P_s (–)	X_m (mol dm^{-3})
(a) Go nanosheets							
0	0.887	0.814	0.168	0	0.887	0.814	0.168
0.1	0.896	0.830	0.179	0.1	0.899	0.834	0.181
0.5	0.904	0.842	0.187	0.5	0.911	0.854	0.197
1	0.913	0.858	0.200	1	0.920	0.870	0.212
2	0.933	0874	0.216	2	0.935	0.894	0.239
3	0.935	0.894	0.239	3	0.950	0.918	0.277
5	0.950	0.918	0.277	5	0.963	0.939	0.330
(b) Functionalized GO nanosheets							
0	0.887	0.814	0.168	0	0.887	0.814	0.168
0.1	0.905	0.842	0.187	0.1	0.911	0.854	0.197
0.5	0.920	0.870	0.212	0.5	0.933	0.890	0.234
1	0.936	0.894	0.239	1	0.948	0.916	0.274
2	0.947	0.914	0.270	2	0.959	0.933	0.313
3	0.956	0.927	0.298	3	0.968	0.948	0.360
5	0.971	0.953	0.380	5	0.981	0.969	0.475

of ions through the membrane is facilitated in narrower passages by creating appropriate channels, and the potential and other transport properties are increased. In the intensive ion traffic, GO nanosheets dominate the ion sites and increase the Donnan exclusion[51,52].

Furthermore, the uniform dispersion of functionalized GO with sulfonic groups in their structure as well as their enhanced water uptake increases the Donnan potential at the two sides of the membrane and thus results in higher transport properties for the corresponded nanocomposite membranes.

The concentration of fixed charges on the membrane surface (X_m) represents a similar trend as the other transport properties of the nanocomposite membranes as seen also in Table 2 and b.

Conductivity

The conductivities of nanocomposite membranes having GO or functionalized GO synthesized by both Hummers and Staudenmaier methods are shown in Figure 13. The figure shows that the conductivity is increased by increasing the filler content as expected. Again, the functionalized GO induces a higher conductivity in either case and the conductivities of nanocomposite membranes having GO or functionalized GO synthesized by Staudenmaier method represent an average of 10–14% higher than the conductivities of nanocomposite membranes having corresponded filler synthesized by Hummers method at the same filler content. The additional pathways of GO, increase in water uptake, and enhancement of chain motion may cause this increase in conductivity for GO nanocomposites, which facilitates the proton conduction through both vehicle and Grotthuss mechanisms[25]. The further increase in proton conductivity of functionalized GO nanocomposites is related to an increase in the membrane's IEC due to the introduction of additional sulfonic acid groups of the functionalized GO. Moreover, the functionalized GO adsorbs water on their surface through a strong interaction with $-SO_3H$ groups and formation of hydrogen bonds and thus increases the water retention and proton conductivity.

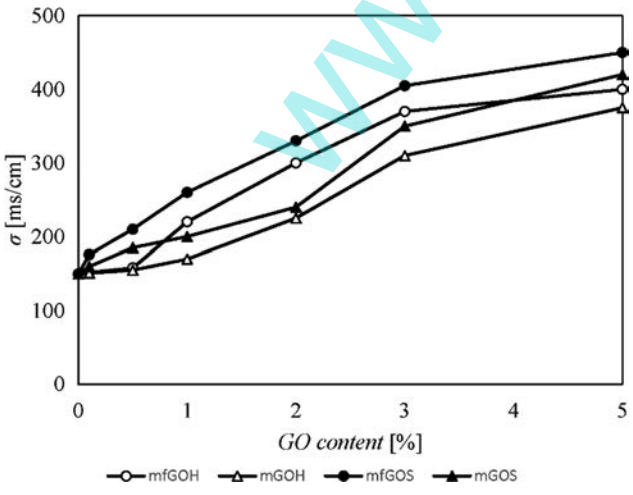

Figure 13. Conductivities of composite membranes having GO synthesized by Staudenmaier and Hummers methods.

The higher conductivities for the nanocomposite membranes having GO or functionalized GO synthesized by Staudenmaier method clearly show that the type of utilized oxidation method has profound influence on the electrochemical properties of the resulting graphene oxide materials, which in turn has eminent implications for any application of graphene oxide in electrochemical devices. In the case of Staudenmaier method, a well-oxidized graphene can be obtained but much longer oxidation time is required. The time for the method proposed by Hummers is shorter, while the graphene oxide possesses a plenty of unoxidized sp^2 carbon atoms[49]. In the two methods, the graphene oxides have comparatively small amounts of carboxyl groups and high amounts of hydroxyl groups. Prolonged drying at ambient temperature allows preserving epoxy groups in the GO obtained from Staudenmaier method that are easily desorbed at slightly higher temperatures[53].

Conclusion

Cation-exchange composite membranes were prepared by introducing various amounts of graphene oxide and fGO nanosheets into the sulfonated PES matrix. The GO nanosheets were prepared by Hummers and Staudenmaier methods. The SEM images of the composite membranes showed a dense structure with uniform distribution of GO nanosheets in the polymeric matrix. The incorporation of GO not only improved the water uptake, thermal, and chemical properties of the composite membranes but also increased their proton conductivities. However, it caused a decrease in the IEC. The chemical interactions between GO and sPES and also the presence of different oxygen functional groups on GO nanosheets enhanced transport properties of GO nanocomposite membranes. Incorporation of functionalized GO in sPES was confirmed to yield a well-distributed composite membrane and to enhance the proton-exchange properties of the membrane. The IEC, water uptake, transport properties, and conductivities of functionalized GO nanocomposite membrane were higher than those of GO nanocomposite membranes and more importantly the functionalized GO synthesized by

Staudenmaier method imparted superior aforementioned properties to the nanocomposite membranes than the functionalized GO synthesized by Hummers method due to the presence of more active sites in the structure of originating GO by the Staudenmaier method. The obtained results make the functionalized GO nanocomposite membranes ideal candidates for utilizing in fuel cells, electrodialysis, and other high-temperature applications.

References

[1] Strathmann, H. Fundumentals in electromembrane separation processes. In: Drioli, E., Giorno, L., eds. *Membrane Operations*, Wiley-VCH: Weinheim, 2009, Chapter 5; pp. 83–88.

[2] Geise, G.M.; Cassady, H.J.; Paul, D.R.; Logan, B.E.; Hickner, M.A.; Logan, E.; Hickner, M.A. Specific ion effects on membrane potential and the permselectivity of ion exchange membranes. Phys. Chem. Chem. Phys. **2014**, *16*, 21673–21681.

[3] Song, M.; Xu, J.; Wu, C. The effect of surface functionalization on the immobilization of gold nanoparticles on graphene sheets. J. Nanotechnol. **2012**, *2012*, 1–5.

[4] Porter, M.C. *Handbook of Industrial Membrane Technology*, Noyes Publications: Park Ridge, NJ, 1988.

[5] Xu, T. Ion exchange membranes: State of their development and perspective. J. Membr. Sci. **2005**, *263*, 1–29.

[6] Hasani-Sadrabadi, M.M.; Dashtimoghadam, E.; Ghaffarian, S.R.; Hasani Sadrabadi, M.H.; Heidari, M.; Moaddel, H. Novel high-performance nanocomposite proton exchange membranes based on poly(ether sulfone). Renew. Energy **2010**, *35*, 226–231.

[7] Thimmappa, R.; Devendrachari, M.C.; Kottaichamy, A. R.; Tiwari, O.; Gaikwad, P.; Paswan, B.; Thotiyl, M.O. Stereochemistry-dependent proton conduction in proton exchange membrane fuel cells. Langmuir **2016**, *32*, 359–365.

[8] Sano, E.; Tanaka, T.; Imai, M. Fabrication and characterization of carbon nanotube/cellulose composite paper. In: Kar, K.K., Pandey, J.K., Rana, S., eds. *Handbook of Polymer Nanocomposites. Processing, Performance and Application*, Vol. B., Springer: Berlin, 2015, Chapter 9; pp. 195–211.

[9] Luo, Z.; Gong, Y.; Liao, X.; Pan, Y.; Zhang, H. Nanocomposite membranes modified by graphene-based materials for anion exchange membrane fuel cells. RSC Adv. **2016**, *6*, 13618–13625.

[10] Çelik, G.; Barsbay, M.; Güven, O. Towards new proton exchange membrane materials with enhanced performance via RAFT polymerization. Polym. Chem. **2016**, *7*, 701–714.

[11] Krishnan, N.N.; Henkensmeier, D.; Jang, J.H.; Kim, H.-J.; Rebbin, V.; Oh, I.-H.; Hong, S.-A.; Nam, S.-W.; Lim, T.-H. Sulfonated poly(ether sulfone)-based silica nanocomposite membranes for high temperature polymer electrolyte fuel cell applications. Int. J. Hydrogen Energy **2011**, *36*, 7152–7161.

[12] Peighambardoust, S.J.; Rowshanzamir, S.; Amjadi, M. Review of the proton exchange membranes for fuel cell applications. Int. J. Hydrogen Energy **2010**, *35*, 9349–9384.

[13] He, Y.; Tong, C.; Geng, L.; Liu, L.; Lü, C. Enhanced performance of the sulfonated polyimide proton exchange membranes by graphene oxide: Size effect of graphene oxide. J. Membr. Sci. **2014**, *458*, 36–46.

[14] Tseng, C.-Y.; Ye, Y.-S.; Cheng, M.-Y.; Kao, K.-Y.; Shen, W.-C.; Rick, J.; Chen, J.-C.; Hwang, B.-J. Sulfonated polyimide proton exchange membranes with graphene oxide show improved proton conductivity, methanol crossover impedance, and mechanical properties, Adv. Energy Mater. **2011**, *1*, 1220–1224.

[15] Hasanabadi, N.; Ghaffarian, S.R.; Hasani-Sadrabadi, M.M. Magnetic field aligned nanocomposite proton exchange membranes based on sulfonated poly(ether sulfone) and Fe_2O_3 nanoparticles for direct methanol fuel cell application. Int. J. Hydrogen Energy **2011**, *36*, 15323–15332.

[16] Kraytsberg, A.; Ein-Eli, Y. Review of advanced materials for proton exchange membrane fuel cells. Energy Fuels **2014**, *28*, 7303–7330.

[17] Gahlot, S.; Sharma, P.P.; Gupta, H.; Kulshrestha, V.; Jha, P.K. Preparation of graphene oxide nano-composite ion-exchange membranes for desalination application. RSC Adv. **2014**, *4*, 24662–24670.

[18] Baker, R.W.; Cussler, E.L.; Eykamp, W.; Koros, W.J.; Riley, R.L.; Strathmann, H. *Membrane Separation System: Recent Developments and Future Directions*, Noyes Data Corporation: New Jersey, 1991.

[19] Klaysom, C.; Moon, S.-H.; Ladewig, B.P.; Lu, G.Q.M.; Wang, L. The effects of aspect ratio of inorganic fillers on the structure and property of composite ion-exchange membranes. J. Colloid Interface Sci. **2011**, *363*, 431–439.

[20] Sata, T. *Ion Exchange Membranes Preparation, Characterization, Modification and Application*, The Royal Society of Chemistry: Cambridge, 2004.

[21] Lo, A.; Huang, C.; Sung, L.; Louh, R. Low humidifying proton exchange membrane fuel cells with enhanced power and Pt-C-h-SiO_2 anodes prepared by electrophoretic deposition. ACS Sustainable Chem. Eng. **2016**, *4*, 1303–1310.

[22] Sheppard, P. Preparation and characterization of composite PES/nanoparticle membranes. B.Sc. Thesis. Worcester Polytechnic Institute, USA, 2013; 40–61.

[23] Kango, S.; Kalia, S.; Celli, A.; Njuguna, J.; Habibi, Y.; Kumar, R. Surface modification of inorganic nanoparticles for development of organic–inorganic nanocomposites—A review. Progr. Polym. Sci. **2013**, *38*, 232–1261.

[24] Zuo, X.; Yu, S.; Xu, X.; Xu, J.; Bao, R.; Yan, X. New PVDF organic–inorganic membranes: The effect of SiO_2 nanoparticles content on the transport performance of anion-exchange membranes. J. Membr. Sci. **2009**, *340*, 206–213.

[25] Su, Y.; Liu, Y.; Sun, Y.; Lai, J.; Wang, D.; Gao, Y.; Liu, B.; Guiver, M. Proton exchange membranes modified with sulfonated silica nanoparticles for direct methanol fuel cells. J. Membr. Sci. **2007**, *296*, 21–28.

[26] Klaysom, C.; Moon, S.H.; Ladewig, B.P.; Lu, G.Q.M.; Wang, L. The influence of inorganic filler particle size on composite ion-exchange membranes for desalination. J. Phys. Chem. C **2011**, *115*, 15124–15132.

[27] Jordan, J.; Jacob, K.I.; Tannenbaum, R.; Sharaf, M.A.; Jasiuk, I. Experimental trends in polymer nanocomposites—A review. Mater. Sci. Eng. A **2005**, *393*, 1–11.
[28] Dreyer D.R.; Park, S.; Bielawski, C.W.; Ruoff, R.S. The chemistry of graphene oxide. Chem. Soc. Rev. **2010**, *39*, 228–240.
[29] Hu, C.; Song, L.; Zhang, Z.; Chen, N.; Feng, Z.; Qu, L. Tailored graphene systems for unconventional applications in energy conversion and storage devices. Energy Environ. Sci. **2014**, *8*, 31–54.
[30] Elangovan, M.; Dharmalingam, S. A facile modification of a polysulphone based anti biofouling anion exchange membrane for microbial fuel cell application. RSC Adv. **2016**, *6*, 20571–20581.
[31] Gahlot, S.; Sharma, P.P.; Kulshrestha, V.; Jha, P.K. SGO/SPES-based highly conducting polymer electrolyte membranes for fuel cell application. ACS Appl. Mater. Interfaces **2014**, *6*, 5595–5601.
[32] Beydaghi, H.; Javanbakht, M.; Kowsari, E. Synthesis and characterization of poly(vinyl alcohol)/sulfonated graphene oxide nanocomposite membranes for use in proton exchange membrane fuel cells (PEMFCs). Ind. Eng. Chem. Res. **2014**, *53*, 16621–16632.
[33] Sun, L.; Fugetsu, B. Massive production of graphene oxide from expanded graphite. Mater. Lett. **2013**, *109*, 207–210.
[34] Deshmukh, K.; Ahamed, M.B.; Shah, A.H.; Pandey, M.; Joshi, G. Morphology, ionic conductivity, and impedance spectroscopy studies of graphene oxide-filled polyvinylchloride nanocomposites. Polym. Plast. Technol. Eng. **2015**, *54*, 1743–1752.
[35] Karim, M.R.; Hatakeyama, K.; Matsui, T.; Takehira, H.; Taniguchi, T.; Koinuma, M.; Matsumoto, Y.; Akutagawa, T.; Nakamura, T.; Noro, S.; Yamada, T.; Kitagawa, H.; Hayami, S. Graphene oxide nanosheet with high proton conductivity. J. Am. Chem. Soc. **2013**, *135*, 8097–8100.
[36] Zarrin, H.; Higgins, D.; Jun, Y.; Chen, Z.; Fowler, M. Functionalized graphene oxide nanocomposite membrane for low humidity and high temperature proton exchange membrane fuel cells. J. Phys. Chem. C **2011**, *115*, 20774–20781.
[37] Rahmanian, A.; Naji, L.; Javanbakht, M. Electrochemical study of the hydrogen adsorption/reduction (HAR) reaction on graphene oxide as an electrocatalyst for proton exchange membrane fuel cells. Iran. J. Hydrogen Fuel Cell **2015**, *2*, 99–107.
[38] Klaysom, C.; Marschall, R.; Wang, L.; Ladewig, B.P.; Lu, G.Q.M. Synthesis of composite ion-exchange membranes and their electrochemical properties for desalination applications. J. Mater. Chem. **2010**, *20*, 4669–4674.
[39] Liu, J.; Xue, Y.; Dai, L. Sulfated graphene oxide as a hole-extraction layer in high-performance polymer solar cells. J. Phys. Chem. Lett. **2012**, *3*, 1928–1933.
[40] Shahriary, L.; Athawale, A.A. Graphene oxide synthesized by using modified Hummers approach. Int. J. Renew. Energy Environ. Eng. **2014**, *2*, 58–63.
[41] Gao, W. Graphite oxide: Structure, reduction and applications. Ph.D. Thesis. Rice University, USA, 2012; 6–7.
[42] Zuo, X.; Yu, S.; Xu, X.; Bao, R.; Xu, J.; Qu, W. Preparation of organic–inorganic hybrid cation-exchange membranes via blending method and their electrochemical characterization. J. Membr. Sci. **2009**, *328*, 23–30.
[43] Peng, S.; Fan, X.; Li, S.; Zhang, J. Green synthesis and characterization of graphite oxide by orthogonal experiment. J. Chil. Chem. Soc. **2013**, *58*, 2213–2217.
[44] Choi, E.-Y.; Han, T.H.; Hong, J.; Kim, J.E.; Lee, S.H.; Kim, H.W.; Kim, S.O. Noncolvalent functionalization of graphene with end-functional polymers. J. Mater. Chem. **2010**, *20*, 1907–1912.
[45] Yu, Y.-H.; Lin, Y.-Y.; Lin, C.-H.; Chan, C.-C.; Huang, Y.-C. High-performance polystyrene/graphene-based nanocomposites with excellent anti-corrosion properties. Polym. Chem. **2014**, *5*, 535–550.
[46] Li, J.; Zeng, X.; Ren, T.; van der Heide, E. The preparation of graphene oxide and its derivatives and their application in bio-tribological systems. Lubricants **2014**, *2*, 137–161.
[47] Paulchamy, B.; Arthi, G.; Lignesh, B.D. A simple approach to stepwise synthesis of graphene oxide nanomaterial. J. Nanomed. Nanotechnol. **2015**, *6*, 2–5.
[48] Thema, F.T.; Moloto, M.J.; Dikio, E.D.; Nyangiwe, N.N.; Kotsedi, L.; Maaza, M.; Khenfouch, M. Synthesis and characterisation of graphene thin films by chemical reduction of exfoliated and intercalated graphite oxide. J. Chem. **2013**, *3*, 1–6.
[49] Ciszewski, M.; Mianowski, A. Survey of graphite oxidation methods using oxidizing mixtures in inorganic acids. Chemik **2013**, *67*, 267–274.
[50] Klaysom, C.; Ladewig, B.P.; Lu, G.Q.M.; Wang, L. Preparation and characterization of sulfonated polyethersulfone for cation-exchange membranes. J. Membr. Sci. **2011**, *368*, 48–53.
[51] Długołecki, P.; Anet, B.; Metz, S.J.; Nijmeijer, K.; Wessling, M. Transport limitations in ion exchange membranes at low salt concentrations. J. Membr. Sci. **2010**, *346*, 163–171.
[52] Farrokhzad, H.; Kikhavani, T.; Monnaie, F.; Ashrafizadeh, S.N.; Koeckelberghs, G.; van Gerven, T.; van der Bruggen, B. Novel composite cation exchange films based on sulfonated PVDF for electromembrane separations. J. Membr. Sci. **2015**, *474*, 167–174.
[53] Poh, H.L.; Šaněk, F.; Ambrosi, A.; Zhao, G.; Sofer, Z.; Pumera, M. Graphenes prepared by Staudenmaier, Hofmann and Hummers methods with consequent thermal exfoliation exhibit very different electrochemical properties. Nanoscale **2012**, *4*, 3515–3522.